Production of strange particles and hypernuclei in spallation reactions from the coupling of intranuclear cascade and de-excitation models

J. Hirtz[*1,2], *J.-C. David*[1], *J.L Rodriguez Sanchez*[1,3,4], *A. Boudard*[1], *J. Cugnon*[5], *S. Leray*[1], *I. Leya*[2], *D. Mancusi*[6] *and G. Schnabel*[1]

[1] IRFU, CEA, Université Paris-Saclay, F-91191, Gif-sur-Yvette, France
[2] Space Research and Planetary Sciences, Physics Institute, University of Bern, 3012 Bern, Switzerland
[3] Universidad de Santiago de Compostela, E-15782 Santiago de Compostela, Spain
[4] GSI-Helmholtzzentrum für Schwerionenforschung GmbH, D-64291 Darmstadt, Germany
[5] AGO department, University of Liège, allée du 6 août 17, bât. B5, B-4000 Liège 1, Belgium
[6] Den-Service d'étude des réacteurs et de mathématiques appliquées (SERMA), CEA, Université Paris-Saclay, F-91191, Gif-sur-Yvette, France

Abstract

Motivated by a renewed interest in hypernucleus studies, the strangeness degree of freedom was implemented in the intranuclear cascade model INCL. This model takes care of the first stage of reactions between a nucleon (or a light cluster) and a nucleus at energies from a few tens of MeV up to a few GeV. After emission of fast particles, a hot remnant nucleus is produced and another model, combined to INCL, handles the de-excitation (the ABLA model in our case). The main ingredients will be discussed and results will be compared to experimental data. The experimental kaon spectra for different target elements and at different energies agree reasonable well with the model predictions. The main remaining discrepancies are analysed and will be explained.

1 Introduction

On the one hand, there is a renew of interest about strangeness physics with new experiments, either in progress or planned, in several worldwide facilities (JPARC, MAMI, JLab, GSI, FAIR, ...). These experiments plan to produce numerous strange particles and notably hypernuclei, which are the best laboratory to study YN and YY interactions. Obviously the light hypernuclei have been studied more extensively than the heaviest ones, but still some questions remain. As examples, we can cite in particular the ${}^{3}_{\Lambda}H$ lifetime, which is shorter than the lifetime of the free Λ, and the Charge Symmetry Breaking observed in the Λ binding energy of the two mirror nuclei ${}^{4}_{\Lambda}H$ and ${}^{4}_{\Lambda}He$ [1]. However, the heavier hypernuclei are also interesting objects to study. They are ideal to study the behaviour of hyperons in nuclear matter and, beyond, to get information on the role of the Λ particles in neutron stars.

On the other hand, there is a nuclear reaction code, called INCL (Liège IntraNuclear Cascade), which treats spallation reactions between light particles and atomic nuclei with incident energies from $\sim 100\ MeV$ up to a few GeV. More precisely, this code handles the first stage of the reaction, leading to an excited nuclear remnant. The de-excitation is usually treated by ABLA, a code often combined to INCL to simulate the entire reaction. INCL, combined to ABLA, is known as a reliable code-combination in the non-strange sector for energies up to 2-3 GeV [2] and, after 2010 with implementation of the multiple pion emission, up to 15 GeV [3].

The renewed interest in strange particle studies and the strong bases of INCL were the motivations to add K's, Λ and Σ's as participant particles in INCL. Most important reactions involving these particles are also included. The de-excitation code ABLA was also upgraded to treat hypernuclei de-excitation

*Corresponding author: jason.hirtz@cea.fr

with evaporation of Λ's and fission of hypernuclei (hyper-fission). Below we give first the ingredients required to perform the calculations and, second, we compare the results obtained to experimental data and to predictions from other model codes. We conclude this paper by summarizing the benchmarking of the code on strange particle emission and on hypernucleus production, with possible improvements.

2 Ingredients

An intranuclear cascade can be summarised to a series of collisions between hadrons. Therefore main ingredients to simulate these collisions are the elementary cross sections (production, scattering, absorption), the final state characteristics of outgoing particles (charges, momenta), the nuclear potential felt by all particles and, possibly, their lifetimes and decay modes. Obviously, other aspects, like Pauli blocking, must be taken into account. It must be stressed that in INCL the resonances are not considered as participant particles (except the $\Delta(1232)$); only their decay products play a role. The reason is threefold. First, the half-lives are short compared to the time between two interactions, second, some resonances overlap and, third, the needed information (cross sections, etc.) are not well known, requiring additional hypotheses.

2.1 Cross sections

Adding the four (anti)Kaons (K^+, K^0, K^-, $\overline{K}^0$), the Λ and the three Σ (Σ^+, Σ^0, Σ^-), calls for hundreds of channels, when isospin is considered. We list below the reactions (isospin not take into account) implemented in INCL. The implementation was done in two steps (Table 1 and Table 2). The second step turned out to be necessary after implementation of the first step.

This short report is not the place to explain all details of how each reaction cross section was determined. This is described in a paper accepted for publication [4]. Here we only draw the attention to the difficulties to obtain all necessary information. As example, the first set, defined in Table 1, includes 382 isospin channels, and therefore as many cross section parametrizations. Only 17% of them were experimentally measured, sometimes very partially. Considering isospin symmetry at the initial and final states, an extra 18% is obtained from relations between known and unknown cross sections. Still relying on isospin symmetry, but working with leading order Feynman diagrams, used within a hadron exchange model, 37% of the cross sections is determined by ratios between known and unknown cross sections. The remaining cross sections are based on models or hypotheses, namely, assuming similarities when a hyperon (kaon) replaces a nucleon (pion). Obviously, the more hypotheses are assumed, less reliable are the reaction cross sections and benchmarking is the only way to know a posteriori the reliability of our model.

NN	$\rightarrow$	$N\Lambda K$	πN	$\rightarrow$	ΛK	$N\overline{K}$	$\rightarrow$	$N\overline{K}$	NK	$\rightarrow$	NK
	$\rightarrow$	$N\Sigma K$		$\rightarrow$	ΣK		$\rightarrow$	$\Lambda\pi$		$\rightarrow$	$NK\pi$
	$\rightarrow$	$N\Lambda K\pi$		$\rightarrow$	$\Lambda K\pi$		$\rightarrow$	$\Sigma\pi$		$\rightarrow$	$NK\pi\pi$
	$\rightarrow$	$N\Sigma K\pi$		$\rightarrow$	$\Sigma K\pi$		$\rightarrow$	$N\overline{K}\pi$	$N\Lambda$	$\rightarrow$	$N\Lambda$
	$\rightarrow$	$N\Lambda K\pi\pi$		$\rightarrow$	$\Lambda K\pi\pi$		$\rightarrow$	$\Lambda\pi\pi$		$\rightarrow$	$N\Sigma$
	$\rightarrow$	$N\Sigma K\pi\pi$		$\rightarrow$	$\Lambda\pi\pi$		$\rightarrow$	$\Sigma\pi\pi$	$N\Sigma$	$\rightarrow$	$N\Lambda$
	$\rightarrow$	$NNK\overline{K}$		$\rightarrow$	$NK\overline{K}$		$\rightarrow$	$N\overline{K}\pi\pi$		$\rightarrow$	$N\Sigma$

Table 1: First set of reactions involving strangeness considered in INCL.

2.2 Final state characteristics

Once a reaction between two hadrons in the nucleus is chosen, charges and momenta of the particles in the final state must be defined. Concerning the charges, Clebsch-Gordan coefficients are used as far as possible if two or more particles are involved. When the number of particles increases, additional models

ΔN	$\rightarrow$	$N\Lambda K$	NN	$\rightarrow$	$K+X$
	$\rightarrow$	$N\Sigma K$			
	$\rightarrow$	$\Delta\Lambda K$	πN	$\rightarrow$	$K+X$
	$\rightarrow$	$\Delta\Sigma K$			
	$\rightarrow$	$NNK\overline{K}$			

Table 2: First set of reactions involving strangeness considered in INCL.

are sometimes needed to remove ambiguities. The reader will find more details in [4]. Otherwise, as in the case of the inclusive reactions listed in the second column of Table 2, results of other codes are used to determine the number and type of particles emitted. Momenta are taken from double differential cross sections, in case measurements exist, or by assuming isotropy or considering phase-space distribution. Here again, the reliability of our approach may differ from channel to channel.

2.3 Average nuclear potentials and decays

While the potential is quite well known for the Λ, the K^+ potential is known to be slightly repulsive and the K^- potential strongly attractive. For Σ's the potential seems to be repulsive, but this is still under debate. For K^0 and $\overline{K}^0$, the same potentials as for K^+ and K^-, respectively, were assumed, but corrected to Coulomb force. The values used in this study are: V_Λ = $-28\ MeV$, V_Σ = 16 MeV, V_K^+ = 25 MeV, V_K^- = $-60\ MeV$, V_K^0 = 15 MeV, $V_{\overline{K}^0}$ = $-50\ MeV$. The latest value implemented in INCL for V_Λ is actually mass dependent. However, the results presented here were performed with the value of $-28\ MeV$, which is very close to the new $V_\Lambda(A)$ for the light and medium mass nuclei except for the figures on hypernuclei de-excitation. Note that, the potential plays a role mainly at low energies.

With half-lives around 10^{-8}-10^{-10} s, none strange particle decays during the cascade, except the Σ^0 (10^{-20} s). The latter point plays a role for Λ and Λ-hypernucleus production rates. After the cascade, the Σ^0 can obviously decay and the K^0 and $\overline{K}^0$ mix to create propagation eigenstate K_s^0 and K_L^0.

3 Results

Comparisons to experimental data and other models are the only way to test the reliability of a model and to try to understand remaining deficiencies. Most of the measured data in this domain are related to the K^+ production. However, some other experimental data exist and were used to benchmark this first version of INCL considering strangeness. Below, figures showing the production of K^+, K^-, K^0, Λ and hypernucleus are shown and analysed.

3.1 K^+ production

Most of the time, K^+ production is well described by INCL. As an example are given two plots (fig. 1) displaying the invariant production cross sections for various angles measured by the KaoS collaboration [5] for different configurations. Either for the left panel with Kaon production near threshold on a light nucleus (carbon) or for the right panel with Kaon production at higher energy on a heavy nucleus (gold), the results of INCL match very well experimental data. Comparison with calculations from the Bertini model [6] implemented in the transport code Geant4 like INCL shows that the INCL model is more than competitive. The difference between both models at low momenta is due to the different K^+ potential values used.

The fig. 2 depicts the production of K^+ with proton projectile from sub-threshold region, with collective effect needed, up to 2.91 GeV on four targets from Be ($Z = 4$) up to Ta ($Z = 73$) is analysed to study the role of the Δ-induced Kaon production by allowing it or not. In the experiment, K^+'s are detected in a very specific phase-space. However, the conclusions are pretty clear. First,

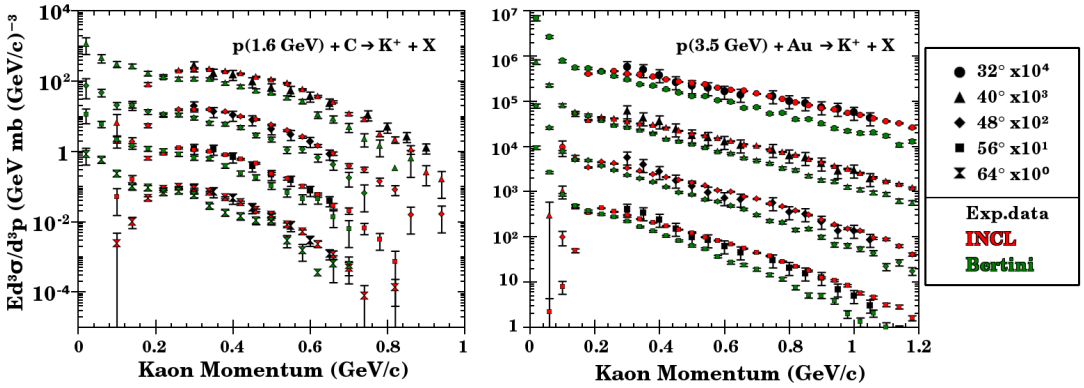

Fig. 1: K^+ invariant production cross sections in $p(1.6\ GeV) + C$ (left) and $p(3.5\ GeV) + Au$ (right) reactions. Experimental data [5] (black) are compared to Bertini [6] (green) and INCL (red)

Δ's play an important role in K^+ production, especially below threshold ($\sim$ 2.1 GeV) and, second, reproduce relatively well ITEP experimental data [7]. Going deeper in the analysis, we can see that INCL slightly overestimates the production with increasing proton energy. This is probably related to the parametrizations used for the Δ-induced Kaon production Ref. [8], where the authors already observed overestimations in some cross section parametrization beyond $\sqrt{s} - \sqrt{s_0} = 200\ MeV$. This is a potential topic to improve.

INCL can also handle heavier projectiles than protons. In fig. 3 are plotted the results obtained for the reaction 2.1 GeV/A in ^{2}H+^{208}Pb. The conclusions are the same as for fig. 1, i.e., INCL matches well the LBL data [9]. Experimental data at lower momenta would help to test the K^+ potential.

With fig. 4, the momentum spectrum is tested in the forward direction. It can be seen the three models plotted, INCL, LAQGSM, and Bertini, fit relatively well experimental data at low momenta. At higher momenta, INCL and LAQGSM reproduce the ANKE data [10] while Bertini underestimates them. Beyond the experimental data, all models have different shapes. Extrapolations from fig. 2 suggest INCL overestimate the real cross section by a factor of roughly 30% for K^+ momentum of 1.28 GeV/c for the configuration of fig. 4. This would be compatible with Bertini's values. Δ-induced kaon production in INCL is probably, here again, overestimated. The same type of data in the entire momentum range

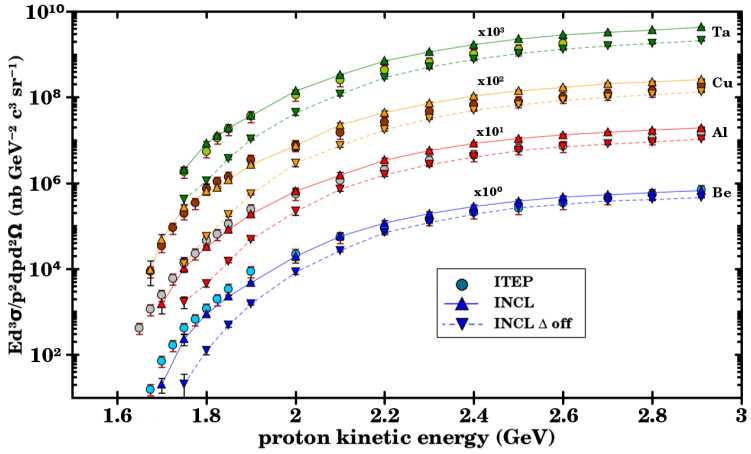

Fig. 2: K^+ production invariant cross section for $p_{K^+} = 1.280 \pm 0.014\ GeV/c$ at $\theta = 10.5°$. Exp. data [7] (circles) are compared to INCL with (up oriented triangles) and without (down oriented triangles) Δ-induced strange production .

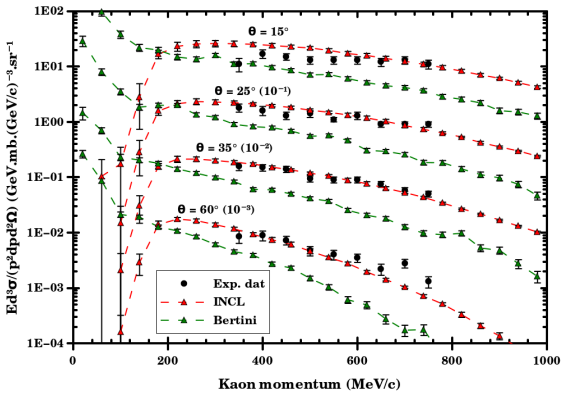

Fig. 3: Kaon production invariant cross section at 2.1 GeV/A in ^{2}H+^{208}Pb collisions. Experimental data [9] (black) are compared to the Bertini cascade model [6] (green) and INCL (red).

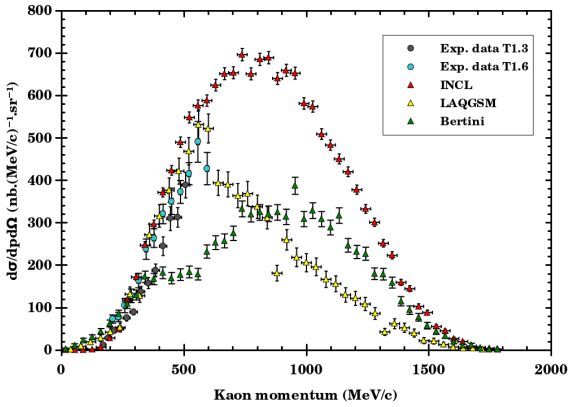

Fig. 4: Forward K^+ spectrum in $p(2.3\ GeV) +^{12} C$ collision. Experimental data [10] (circles) are compared to INCL (red), LaQGSM [11] (yellow) and the Bertini cascade model [6] (green).

would help to better understand the mechanisms involved.

Most of experiment on strangeness production are carried out with projectile energies between 1.5 and 3.5 GeV. However, INCL is designed to do calculation up to 15 GeV. Fig. 5 allows tests for the highest energies with a projectile momentum of 14.6 GeV/c ($T \simeq 13.7\ GeV$). The rapidity spectra for the four targets exhibit good simulation of INCL at high energies. However, an underestimation at high rapidity for the heaviest targets could be observed.

While fig. 5 deals with high energies, fig. 6 tests the lowest energies with the far sub-threshold K^+ production. The threshold for the K^+ production in proton-proton collision is around 1580 MeV. Here, energies are much below, which imply strong collective effects. The first observation, which can be done, is the overestimation by a factor 4 of the experimental data. However, we observed also the slops are relatively well reproduced. Drawing a conclusion from this figure is extremely hard because of the complexity of the sub-threshold K^+ production processes.

In addition to the physical analysis, fig. 6 was a good opportunity to test a novelty in INCL: the biasing. Production rates of strange particles are much lower than those of *non-strange* particles, resulting in a dramatical increase of computation time. However, this has been mitigated by introducing

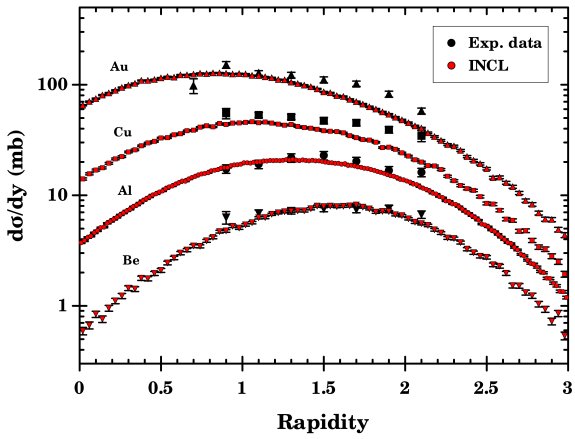

Fig. 5: K^+ rapidity spectrum in $p(14.6\ GeV/c) + A$ collision. The experimental data are from [12].

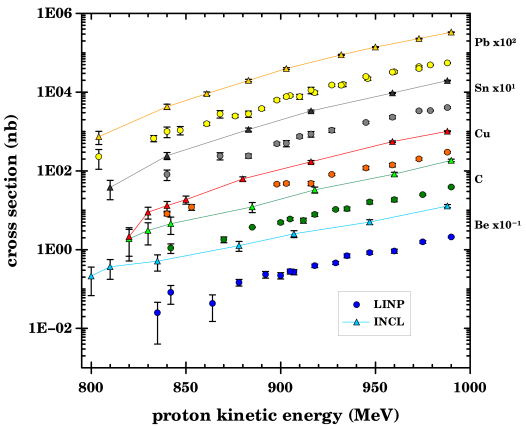

Fig. 6: Subthreshold K^+ production cross section in $p + A$ collision. Experimental data from [13]

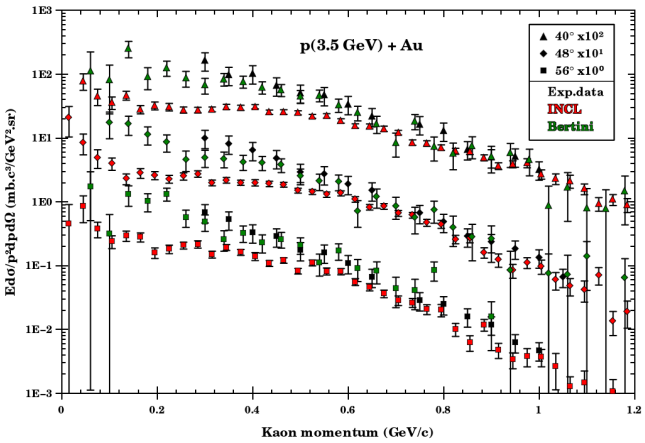

Fig. 7: K^- invariant cross section in $p(3.5\ GeV) + Au$ collision. Experimental data [5] (black) are compared to Bertini (green) and INCL (red).

a biasing process in INCL. Calculation times needed to obtain good statistics for strange particles are now reasonable. Here, the conditions are excellent. As a result, the biasing reduced by a factor between 1000 and 2000 the time needed to get this figure.

3.2 K^- production

The conclusions for the K^- differ from the conclusions above for the K^+. The spectra on fig. 7 are well reproduced except for low momenta. In this region the Bertini code gives better results, what seems to indicate that in INCL some production channels are missing, especially the $YN \rightarrow \overline{K}NN$. This corroborates the state made in Ref. [5], arguing that the role of strangeness exchange reactions was important in K^- production.

3.3 Neutral kaon production

AntiKaon production is marginal compared to Kaon production. Therefore, physics associated to neutral kaons in experiments are dominated by the K^0 production, which is strongly correlated to K^+ production. Considering this, results as good as for K^+ are expected. However, comparisons with experimental data show significant discrepancies.

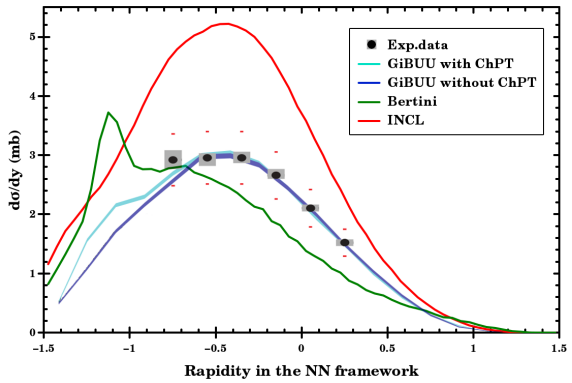

Fig. 8: K^0_s rapidity distribution in $p(3.5\ GeV) + Nb$ collisions. HADES data [14] (black) are compared to GiBUU (blue), Bertini (green), and INCL (red).

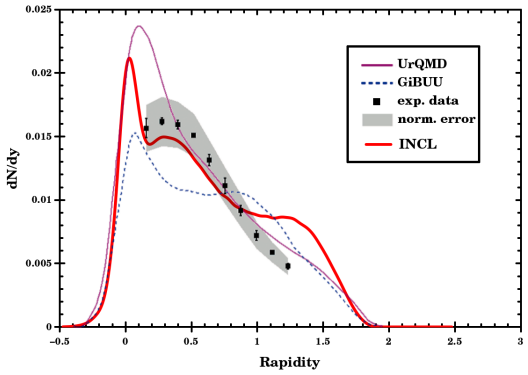

Fig. 9: Λ rapidity in $p(3.5\ GeV) + Nb$ collisions. HADES data [16] (black) are compared to UrQMD (purple), GiBUU (blue), and INCL (red).

On fig. 8, the shape of INCL is good but the calculation overestimates experimental data [14] by roughly 40%. As for K^+ production, Δ-induced production could be an explanation, but another reason can be put forward: the total reaction cross section $\sigma_{tot}^{p\ Nb}$ measured by HADES is $848 \pm 127\ mb$, while INCL calculates a value of $1048\ mb$. A measurement of the total reaction cross section for the same system at a lower energy ($1.2\ GeV$ instead of $3.5\ GeV$) gave $1063 \pm 40\ mb$ [15]. Therefore, a part of the overestimation is probably due to the normalization.

3.4 Λ production

The production of hypernuclei is strongly connected to the production of Λ, since most of the observed hypernuclei are involving a Λ. Therefore, before studying the hypernucleus production, we tested our model for the Λ production. Once again, experimental data are very scarce and we can only show one diagram. We compared the INCL results to the HADES rapidity spectrum for the reaction $p(3.5GeV) + Nb$ (fig. 9), as well as to some other models. INCL matches rather well the HADES data [16], except for rapidities larger than 0.8. The bump seen with INCL around $y = 1.3$, but not with the HADES data, also exists for the GiBUU model [17], but at lower rapidities. The UrQMD model [18] does not exhibit such a behaviour and is close to HADES, but misses strongly the two data points at low rapidity. The shape of the rapidity spectrum beyond 0.8 is possibly due to the low transverse momenta, but a careful study must be carried out to understand the differences between experimental data and model predictions.

3.5 Hypernucleus production

While single strange particle production is dominated by the intranuclear cascade and can be described by INCL alone, hypernucleus production is strongly dependent on both processes, the intranuclear cascade and the de-excitation. Comparisons with experimental data require so a combination of INCL and ABLA.

Here, two types of plots are displayed. The fig. 10 shows the isobaric production of hypernuclei by π^+-induced reactions (${}^A X(\pi^+, K^+)^A_\Lambda X$) as a function of the mass target. It can be seen INCL-ABLA fits very well the KEK experimental data [20]. Initially, INCL-ABLA underestimated the KEK data for the two heaviest nuclei. This led us to consider an Λ potential dependant on the nucleus mass [19]. The thus updated INCL model produces a perfect fit of the measurements. Another conclusion is the crucial role played by the de-excitation code, reducing the production rate by more than one order of magnitude compared to the rate at the end of the cascade. This latter result gives the probability that the

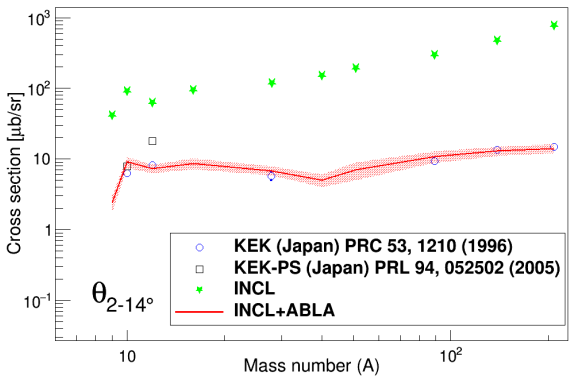

Fig. 10: Hypernucleus production cross section in function of the mass target for ${}^A X(\pi^+, K^+)^A_\Lambda X$ reactions, with incident energies of 1.06 and 1.048 GeV/c. Experimental data are from [20](circles) and [21] (squares). Are plotted INCL hyper-remnant production (green stars) and INCL-ABLA result (red line)

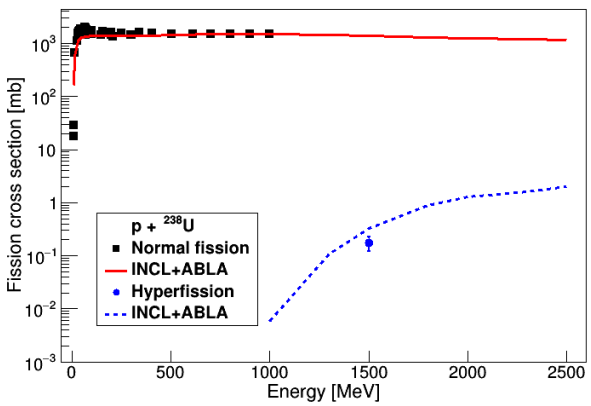

Fig. 11: Fission and hyper-fission cross sections in function of the proton projectile energy in p+U. *Normal* fission [22] and hyper-fission [23] experimental data are compared to INCL-ABLA results (red line and dotted-blue line respectively).

Λ particle does not evaporate and the ABLA code, upgraded on purpose, describes well the de-excitation of hypernuclei.

In fig. 11, the fission of hypernuclei is tested. At the end of the intranuclear cascade, if the target is heavy enough, the remnant can undergo fission. This remnant can be a hypernucleus or not. For *normal* nuclei, we know that the combination INCL-ABLA gives good results, as shown in fig. 11. With the implementation of hyper-fission in ABLA, in particular by taking into account hyper-energy in the fission barrier height, we conclude that ABLA is able to calculate a hyper-fission cross section very close to the rare experimental data.

4 Conclusion

The strange particles K^+, K^-, $\overline{K}^0$, K^-, Λ, Σ^+, Σ^0 and Σ^- are implemented into the intranuclear cascade code INCL. Since the de-excitation code ABLA is usually combined to INCL for a full simulation of spallation reactions, ABLA has also been upgraded by adding Λ evaporation and hyper-fission. Results obtained by the codes, and especially INCL, are very encouraging. Main mechanisms are incorporated and now it is time for improvements. Δ-induced strangeness production is probably overestimated when energy goes up and some strangeness exchange reactions must be added, like $\Lambda N \rightarrow \overline{K}NN$, to better reproduce antiKaon production. Other aspects must also be studied, like the momentum distribution of the emitted particles. However, the lack of experimental data to get better elementary ingredients and to benchmark carefully our model makes the task difficult.

References

[1] C. Rappold, T.R.Sait et al., Physics Letters B 728, 543-548 (2014)

[2] S. Leray et *al.*, J. Korean Phys. Soc. 59, 791-796 (2011) IAEA Benchmark of Spallation Models

[3] S. Pedoux and J. Cugnon, Nucl. Phys. A 866, 16-36 (2011)

[4] J. Hirtz, J.C. David et al., arXiv:1805.01655 [nucl-th] (2018)

[5] W. Scheinast et al., PRL 96, 072301 (2006)

[6] D.H. Wright, M.H. Kelsey, NIM in Physics Research A 804, 175-188 (2015)

[7] A.V. Akindinov et al., JETP Letters, Vol. 72, 100 (2000)

[8] K. Tsushima, A. Sibirtsev, A. W. Thomas, and G. Q. Li, Phys. Rev. C 59, 369 (2000), Erratum.

[9] S. Schnetzer, R. M. Lombard et al., Phys. Rev. C 40, 640 (1990), Erratum

[10] Büscher, M., Koptev, V., Nekipelov, M. et al., Eur. Phys. J. A 22, 301 (2004)

[11] N.V. Mokhov, K.K. Gudima, S.I. Striganov., arXiv:1409.1086 [nucl-ex] (2014)

[12] T. Abbott et al. (E-802 Collaboration), Phys. Rev. D 45, 3906 (1992).

[13] V.P. Koptev et al., Zh. Eksp. Teor. Fiz. 94,1-14 (1988).

[14] HADES Collaboration, Phys. Rev. C 90, 054906 (2014)

[15] C.-M. Herbach et al., Nucl. Instr. Meth. A 562, 729 (2006)

[16] HADES Collaboration, Eur. Phys. J. A 50, 81 (2014)

[17] O. Buss and all. Physics Reports 512, 1-124 (2012)

[18] S. A. Bass et al., arXiv:nucl-th/9803035v2

[19] J. L. Rodríguez-Sánchez, J.-C. David, J. Hirtz, J. Cugnon, and S. Leray Phys. Rev. C 98, 021602 (2018)

[20] T. Hasegawa and al., Phys. Rev. C 53, 1210 (1996)

[21] P. K. Saha et al. Phys. Rev. Lett. 94, 052502 (2005)

[22] IAEA EXFOR data base, https://www-nds.iaea.org/exfor/exfor.htm

[23] P. Kulessa et al., Physics Letters B 427, 403-408 (1998)